AMERICAN SOCIETY FOR MICROBIOLOGY | Applied and Environmental Microbiology®

GEOMICROBIOLOGY

Unraveling Fe(II)-Oxidizing Mechanisms in a Facultative Fe(II) Oxidizer, *Sideroxydans lithotrophicus* Strain ES-1, via Culturing, Transcriptomics, and Reverse Transcription-Quantitative PCR

Nanqing Zhou,[a] Jessica L. Keffer,[b] Shawn W. Polson,[c,d] Clara S. Chan[a,b]

[a]School of Marine Science and Policy, University of Delaware, Newark, Delaware, USA
[b]Department of Earth Sciences, University of Delaware, Newark, Delaware, USA
[c]Department of Computer and Information Sciences, University of Delaware, Newark, Delaware, USA
[d]Center for Bioinformatics and Computational Biology, University of Delaware, Newark, Delaware, USA

ABSTRACT *Sideroxydans lithotrophicus* ES-1 grows autotrophically either by Fe(II) oxidation or by thiosulfate oxidation, in contrast to most other isolates of neutrophilic Fe(II)-oxidizing bacteria (FeOB). This provides a unique opportunity to explore the physiology of a facultative FeOB and constrain the genes specific to Fe(II) oxidation. We compared the growth of *S. lithotrophicus* ES-1 on Fe(II), thiosulfate, and both substrates together. While initial growth rates were similar, thiosulfate-grown cultures had higher yield with or without Fe(II) present, which may give ES-1 an advantage over obligate FeOB. To investigate the Fe(II) and S oxidation pathways, we conducted transcriptomics experiments, validated with reverse transcription-quantitative PCR (RT-qPCR). We explored the long-term gene expression response at different growth phases (over days to a week) and expression changes during a short-term switch from thiosulfate to Fe(II) (90 min). The *dsr* and *sox* sulfur oxidation genes were upregulated in thiosulfate cultures. The Fe(II) oxidase gene *cyc2* was among the top expressed genes during both Fe(II) and thiosulfate oxidation, and addition of Fe(II) to thiosulfate-grown cells caused an increase in *cyc2* expression. These results support the role of Cyc2 as the Fe(II) oxidase and suggest that ES-1 maintains readiness to oxidize Fe(II), even in the absence of Fe(II). We used gene expression profiles to further constrain the ES-1 Fe(II) oxidation pathway. Notably, among the most highly upregulated genes during Fe(II) oxidation were genes for alternative complex III, reverse electron transport, and carbon fixation. This implies a direct connection between Fe(II) oxidation and carbon fixation, suggesting that CO_2 is an important electron sink for Fe(II) oxidation.

IMPORTANCE Neutrophilic FeOB are increasingly observed in various environments, but knowledge of their ecophysiology and Fe(II) oxidation mechanisms is still relatively limited. *Sideroxydans* isolates are widely observed in aquifers, wetlands, and sediments, and genome analysis suggests metabolic flexibility contributes to their success. The type strain ES-1 is unusual among neutrophilic FeOB isolates, as it can grow on either Fe(II) or a non-Fe(II) substrate, thiosulfate. Almost all our knowledge of neutrophilic Fe(II) oxidation pathways comes from genome analyses, with some work on metatranscriptomes. This study used culture-based experiments to test the genes specific to Fe(II) oxidation in a facultative FeOB and refine our model of the Fe(II) oxidation pathway. We gained insight into how facultative FeOB like ES-1 connect Fe, S, and C biogeochemical cycling in the environment and suggest a multigene indicator would improve understanding of Fe(II) oxidation activity in environments with facultative FeOB.

KEYWORDS *Sideroxydans lithotrophicus*, *cyc2*, iron oxidation, sulfur oxidation, transcriptomics

Editor Nicole R. Buan, University of Nebraska—Lincoln

Address correspondence to Clara S. Chan, cschan@udel.edu.

The authors declare no conflict of interest.

Received 16 August 2021
Accepted 11 November 2021
Accepted manuscript posted online 17 November 2021
Published 25 January 2022

Neutrophilic Fe(II)-oxidizing bacteria (FeOB) are increasingly found in a wide variety of terrestrial and marine environments (1–4), often in suboxic zones where microaerophilic FeOB can successfully outcompete Fe(II) oxidation by oxygen (5, 6). In these environments, FeOB have the potential to affect many elemental cycles, notably carbon cycling, as many neutrophilic FeOB are autotrophic and sequester organics in their biominerals (7, 8). The most well-characterized neutrophilic FeOB are the marine *Zetaproteobacteria* and freshwater/terrestrial *Gallionellaceae* (2, 9, 10), though our knowledge of both remains limited. There are relatively few isolates, and most are obligate Fe(II) oxidizers. FeOB are relatively difficult to culture, and the resulting iron oxides interfere with many standard molecular techniques, such as nucleic acid extraction and assays. These ongoing challenges have limited our understanding of Fe(II) oxidation mechanisms and ecophysiology of facultative FeOB.

Within the *Gallionellaceae*, *Sideroxydans* is a genus of microaerophilic Fe(II) oxidizers widespread in terrestrial aquatic systems, including groundwater, wetlands, creek sediments, and rhizosphere soil (11–16). *Sideroxydans* isolates have been identified from moderately acidic to circumneutral environments, over a wide range of oxygen concentrations (17–20), commonly in environments with both high Fe and S concentrations (21–23). The type strain is *Sideroxydans lithotrophicus* ES-1, isolated from groundwater using FeS and O_2, with growth over a pH range of 5.5 to 7.5 (24). ES-1 is able to grow on Fe(II) or thiosulfate, making it unusual among neutrophilic FeOB in that it is a facultative Fe(II) oxidizer. The strain has a fully sequenced, closed genome that encodes multiple putative Fe(II) oxidases (25), suggesting further metabolic flexibility. The metabolic versatility makes ES-1 a good model to study the physiology of a facultative FeOB, compare the expression of different putative Fe(II) oxidase genes, and investigate genes that are specifically involved in Fe(II) oxidation.

The ES-1 genome includes multiple potential pathways for both S and Fe oxidation. The sulfur oxidases encoded in the ES-1 genome are thiosulfate dehydrogenase (Tsd), reverse dissimilatory sulfite reductase (rDsr), and sulfur oxidase (Sox). The two main putative Fe(II) oxidases in ES-1 are Cyc2 and MtoA (25, 26). Cyc2 is the homolog of the Fe(II) oxidase identified in *Acidithiobacillus ferrooxidans* (27) and *Mariprofundus ferrooxydans* (28), and it is widely distributed in microaerophilic FeOB (26, 29). MtoA is the homolog of the decaheme Fe(III) reductase MtrA in *Shewanella oneidensis* and showed Fe(II) oxidation activity *in vitro* (30). MtoA is part of a gene cluster that also encodes a porin (MtoB), a putative periplasmic cytochrome (MtoD), and an inner membrane electron shuttle (CymA) (25, 30). Previous research suggests microaerophilic Fe(II) oxidation occurs extracellularly (31–33), which requires periplasmic electron carriers to transfer electrons from Cyc2 or MtoA to terminal oxidases or complex I through the reverse electron transfer (RET) chain (8, 31, 33). Genomic analysis of ES-1 has revealed genes that encode different parts of the potential electron transfer pathways, including cbb_3 and *bd* cytochrome oxidases as the terminal oxidases, bc_1 complex and alternative complex III (ACIII) as complex III, NADH dehydrogenase (complex I), and succinate dehydrogenase (complex II) (25). Moreover, ES-1 contains genes for two forms of RuBisCO, which would enable it to efficiently fix CO_2 under different environmental conditions (25). However, since no ES-1 transcriptomics or proteomics has been performed, the Fe(II) oxidation pathway has not been verified. In particular, it is still unknown if *cyc2* and *mtoA* are specifically involved in Fe(II) oxidation, and the role of ACIII and other cytochromes has been speculative.

In this study, we used physiological, transcriptomic, and reverse transcription-quantitative PCR (RT-qPCR) approaches to study the metabolism and metabolic pathways of ES-1 using different substrates. Growth was characterized on Fe and S substrates individually, in series (i.e., substrate switching), and together. Transcriptomes of ES-1 grown on Fe(II) [Fe(II)-citrate and $FeCl_2$] or thiosulfate were sequenced to look at the long-term (days) and short-term (minutes to hours) responses to different electron donors. Differential gene expression (DGE) analysis was used to constrain genes specific to Fe(II) oxidation. RT-qPCR was used to further quantify the expression of *cyc2*

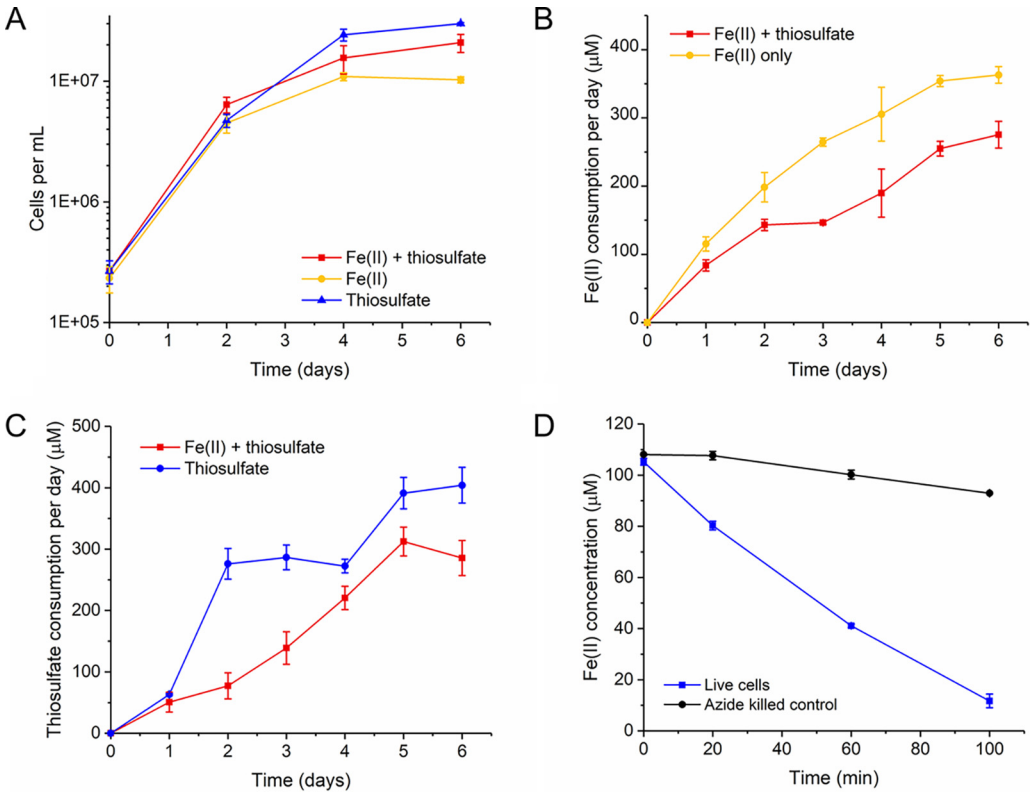

FIG 1 (A) ES-1 growth on $FeCl_2$-only, thiosulfate-only, or $FeCl_2$ plus thiosulfate culture. (B) Biotic Fe(II) consumption per day in $FeCl_2$-only culture and $FeCl_2$ plus thiosulfate culture. (C) Biotic thiosulfate consumption per day in thiosulfate-only culture and $FeCl_2$ plus thiosulfate culture. (D) Fe(II) concentration change after spiking $FeCl_2$ (100 μM) into stationary-phase thiosulfate-grown culture. The Fe(II) and thiosulfate consumption values were calculated using the concentration after $FeCl_2$ and thiosulfate supplement on day n subtracted by the $FeCl_2$ and thiosulfate concentration before supplementation on day $n + 1$. To calculate biotic consumption, the abiotic consumption was subtracted from culture consumption values.

and *mtoA* under different conditions. With these results, we gained insight into the physiology of a metabolically flexible Fe(II) oxidizer, clarified the roles of potential Fe(II) oxidase genes, and improved the current Fe(II) oxidation electron transfer pathway model in a facultative microaerophilic FeOB.

RESULTS

Characterizing ES-1 growth on different substrates. We compared ES-1 growth on thiosulfate or $FeCl_2$ individually and when both substrates were available concurrently. We grew ES-1 cultures with a daily amendment of only $FeCl_2$, only thiosulfate, or both $FeCl_2$ and thiosulfate at a daily target concentration of 500 μM since that concentration results in the highest ES-1 biomass yield on $FeCl_2$. Cell growth rates were initially comparable (slightly faster on $FeCl_2$ plus thiosulfate at day 2), but ultimately, the cell concentration in the thiosulfate-only culture was the highest (Fig. 1A). The only thiosulfate oxidation product was tetrathionate (see Fig. S1 in the supplemental material); thus, in ES-1, Fe(II) oxidation and thiosulfate oxidation are both one-electron reactions. The electron uptake rate at mid-log phase was 3.7×10^{-8} to 3.8×10^{-8} μmol e^-/cell/day in the cultures with single substrates, which was slightly higher than the culture with both substrates (2.9×10^{-8} μmol e^-/cell/day). When both substrates were present, cells consumed Fe(II) and thiosulfate simultaneously, suggesting there is no preference under these growth conditions (red lines in Fig. 1B and C). However, there was a lag in thiosulfate consumption at day 1 (blue line in Fig. 1C), perhaps due to the fact that the inoculum was pregrown on $FeCl_2$. To investigate if thiosulfate-grown cells would show a lag in Fe(II) oxidation when switched back to

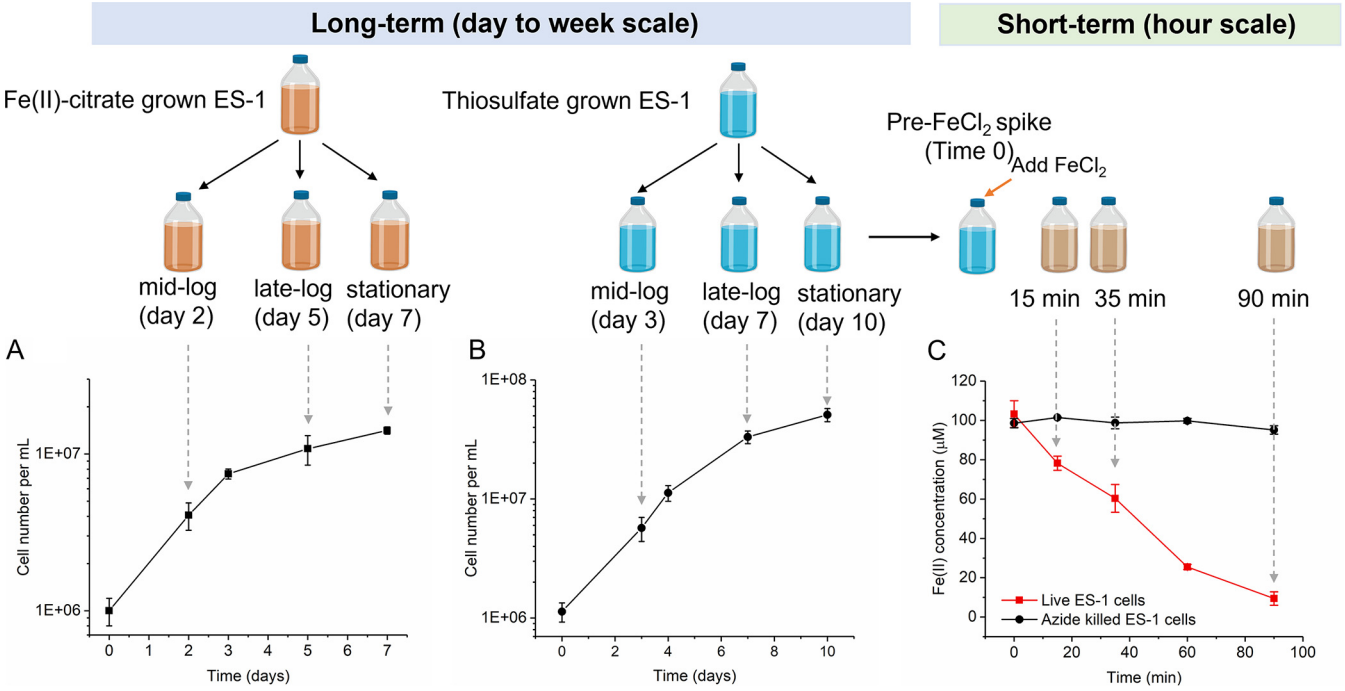

FIG 2 (A) Growth of ES-1 with daily feeding of 500 μM Fe(II)-citrate. (B) Growth of ES-1 on one-time dose of 10 mM thiosulfate; (C) Fe(II) oxidation kinetics after $FeCl_2$ spike into stationary thiosulfate culture. Gray arrows indicate the sample points.

$FeCl_2$, we grew ES-1 on thiosulfate and then spiked in $FeCl_2$. In this case, there was no lag, as thiosulfate-grown ES-1 started to oxidize Fe(II) immediately, while the azide-killed control showed negligible Fe(II) oxidation, demonstrating that the Fe(II) oxidation was nearly all biotic (Fig. 1D). The lag from Fe(II) oxidation to thiosulfate oxidation (but not the reverse) suggests that ES-1 maintains readiness to oxidize Fe(II) but regulates its ability to oxidize thiosulfate.

Growing ES-1 on $FeCl_2$ yields copious oxyhydroxides, which can interfere with RNA extraction. We therefore evaluated the growth of ES-1 on Fe(II)-citrate, as citrate would chelate Fe(III) and prevent mineral formation, but not affect Fe(II) oxidation kinetics (34). ES-1 can grow on Fe(II)-citrate without forming Fe(III) oxyhydroxides but showed no growth on citrate alone, demonstrating that growth was due to Fe(II) oxidation (see Fig. S2A in the supplemental material). We optimized cell growth on Fe(II)-citrate and thiosulfate by trying a series of substrate concentrations (from 100 to 750 μM Fe(II) per day, with one-time addition of 0.5 to 10 mM thiosulfate) (Fig. S2A and S2B). The growth data showed that when cultures were dosed with similar amounts of Fe(II)-citrate and thiosulfate, yield on thiosulfate was higher. From these results, we chose an Fe(II)-citrate concentration of 500 μM per day and a thiosulfate concentration of 10 mM to maximize the biomass yield on each substrate.

Transcriptome analysis revealed genes used during Fe(II) and thiosulfate oxidation. To investigate genes involved in Fe(II) and thiosulfate oxidation, we conducted long-term single-substrate experiments and a short-term Fe(II) addition experiment. In the long-term experiment (7 to 10 days), cells were grown on either Fe(II)-citrate or thiosulfate, and samples were taken from different growth phases: mid-log, late-log, and early stationary phase (Fig. 2A and B). To analyze differential gene expression, pairs of time points were compared [for example, mid-log on Fe(II)-citrate to mid-log on thiosulfate]. To investigate the short-term response of ES-1 to Fe(II), we spiked $FeCl_2$ into an ES-1 culture grown on thiosulfate and collected samples at the early (15 min), middle (35 min), and the end (90 min) of the Fe(II) oxidation curve, along with a pre-$FeCl_2$ spike (time zero) control for comparison (Fig. 2C). Citrate was not necessary for short-term experiments since relatively little Fe(III) oxyhydroxide is formed. In this short-term experiment, gene expression at each time point (15, 35, and 90 min) was

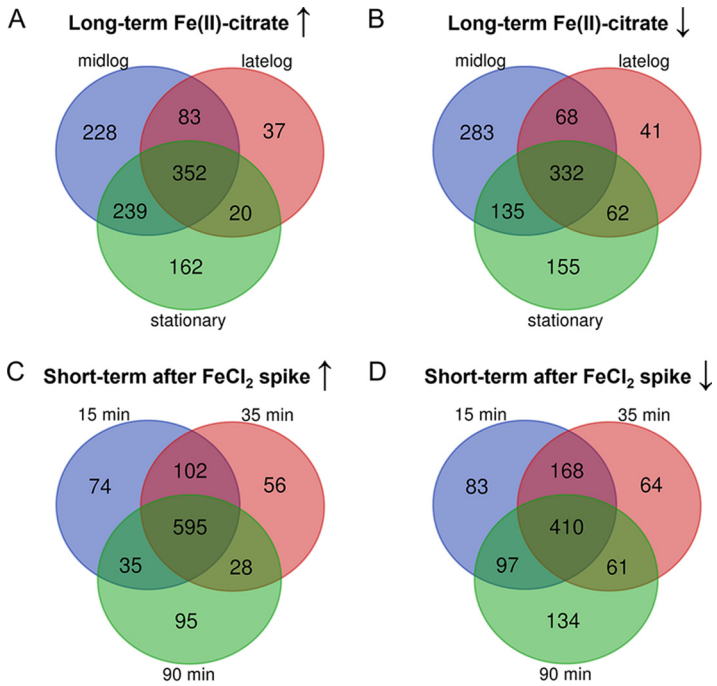

FIG 3 Venn diagram of (A) upregulated genes and (B) downregulated genes in long-term Fe(II)-citrate compared to thiosulfate culture at different growth phases. (C) Upregulated genes and (D) downregulated genes at different time points after adding $FeCl_2$ compared to time zero (stationary thiosulfate-grown culture) ($P \leq 0.05$).

compared to that of the thiosulfate-grown stationary cells (time zero). All gene expression values are presented as transcripts per million (TPM), normalized by dividing by the average TPM of six constitutively expressed genes (*gyrB*, *gyrA*, *adk*, *rho*, *era*, and *gmk*) (35).

Clear differences in gene expression were evident between growth on Fe(II)-citrate and thiosulfate in both long- and short-term experiments from the differential gene expression (DGE) analyses. Mid-log phase represented the largest difference between Fe(II)-citrate and thiosulfate cultures, as can be seen from the high number of genes differentially expressed during this time point (Fig. 3A and B). In the short-term response, the number of genes differentially expressed was the highest at 90 min (Fig. 3C and D). We explored the differentially expressed genes to constrain the genes involved in ES-1 metabolism on different substrates.

Expression and regulation of thiosulfate oxidases. ES-1 has several thiosulfate oxidation pathways, including Tsd (*tsdAB*; Slit_1878 to Slit_1877), Dsr (*dsrPOJLKMCHFEBA*; Slit_1675 to Slit_1686), and Sox (*soxBAXYZ*; Slit_1696 to Slit_1700). Each pathway could produce a different oxidation product, including tetrathionate, elemental sulfur, or sulfate (36). The only thiosulfate oxidation product generated by ES-1 is tetrathionate; no other oxidation products such as S(0) or sulfate were detected (Fig. S1). This suggests the use of *tsdAB* to convert thiosulfate to tetrathionate, since Sox and Dsr pathways are not known to oxidize thiosulfate to tetrathionate (37). However, our transcriptome data showed *tsdAB* genes were neither upregulated nor highly expressed in thiosulfate culture, while *sox* and *dsr* gene clusters were highly expressed and significantly upregulated during thiosulfate growth (Fig. 4; see Table S1 in the supplemental material).

Expression and regulation of potential Fe(II) oxidases. We examined the possible Fe(II) oxidation genes by transcriptomics and further validated the transcriptome sequencing (RNA-Seq) results by RT-qPCR. ES-1 has three *cyc2* genes adjacent to one another in the genome, separated by 604- and 437-bp intergenic regions and preceded by transcriptional regulators (see Fig. S3 in the supplemental material). The three *cyc2* genes are not identical because their amino acid identity varies from 37% to

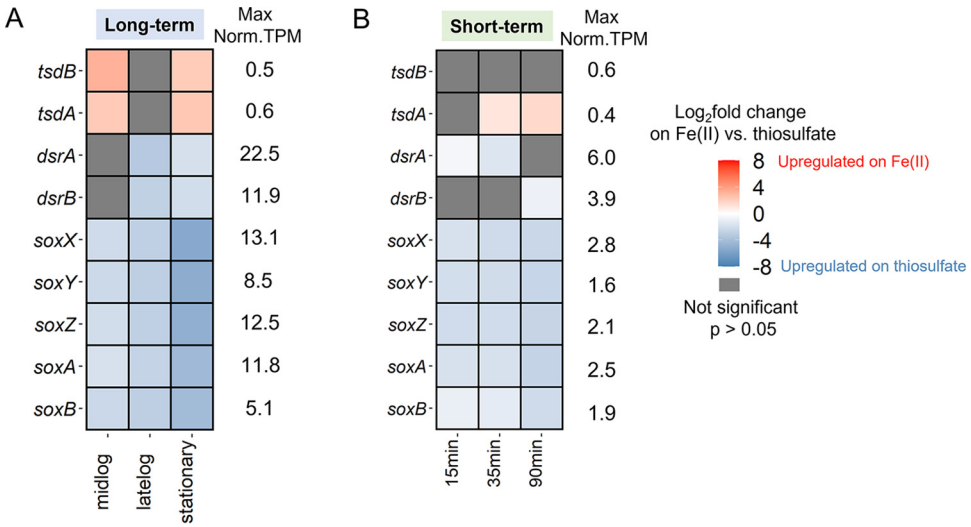

FIG 4 Differential gene expression and maximum constitutive normalized TPM of possible thiosulfate oxidase genes in the (A) long-term and (B) short-term experiments. In the long-term experiment, the reference is thiosulfate-grown ES-1 at different growth phases; in the short-term experiment, the reference is time 0 (stationary thiosulfate-grown ES-1). Blue corresponds to upregulation on thiosulfate.

50%. Each of the four genes (three *cyc2* genes and *mtoA*) behaved differently in response to Fe(II). Overall, the RT-qPCR results compared to the transcriptome showed slightly higher relative expression level than the constitutive normalized TPM values (see Tables S2 and S3 in the supplemental material), but the expression patterns from the two methods were in agreement. In all cultures, *cyc2* expression was generally higher than *mtoA* expression (Fig. 5). In Fe(II)-citrate culture, where the Fe(II)-oxidizing-related genes should be expressed, the RT-qPCR result shows the three *cyc2* genes were expressed on average 359-, 70-, and 21-fold higher than *mtoA* ($P \leq 0.01$, Student's *t* test) (Fig. 5A; Table S2), while the values calculated from constitutive normalized TPM were 1,180-, 467-, and 157-fold. Among the three *cyc2* genes, *cyc2_1* showed the highest expression and is one of the top expressed genes under all conditions (Fig. 5; Table S3). This result suggests that *cyc2* plays a larger role in Fe(II) oxidation than *mtoA* under the conditions tested.

The individual responses to Fe(II) varied for each of the three *cyc2* genes. The RT-qPCR results show *cyc2_1* increased in expression level from 106.31 to 145.23 in

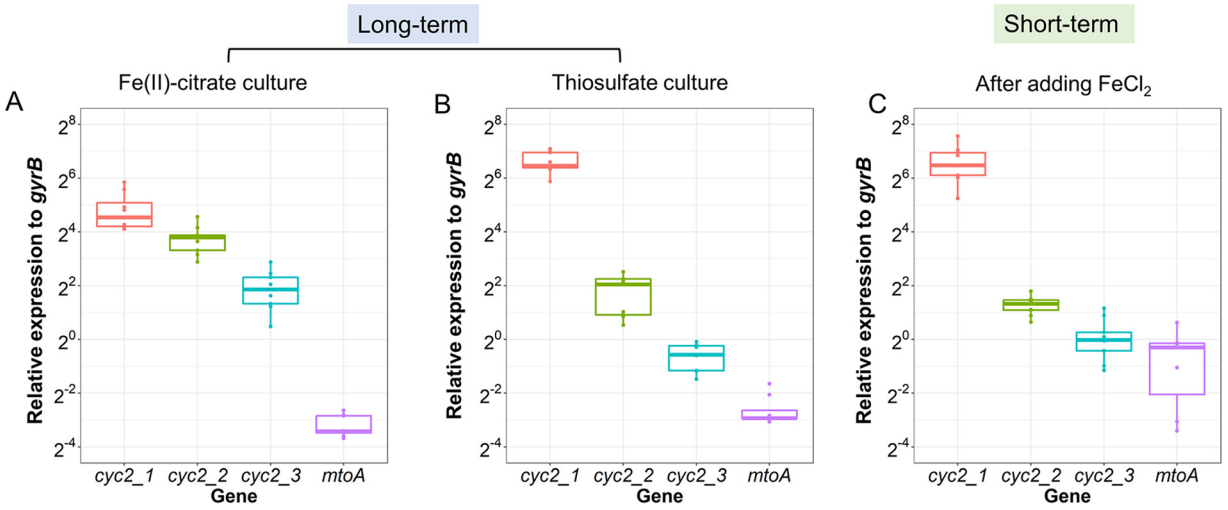

FIG 5 Expression level of the four putative Fe(II) oxidase genes by RT-qPCR in (A) long-term Fe(II)-citrate culture, (B) long-term thiosulfate culture, and (C) short-term culture after adding $FeCl_2$. Error bars show the 95% confidence interval; the line inside the box is the median.

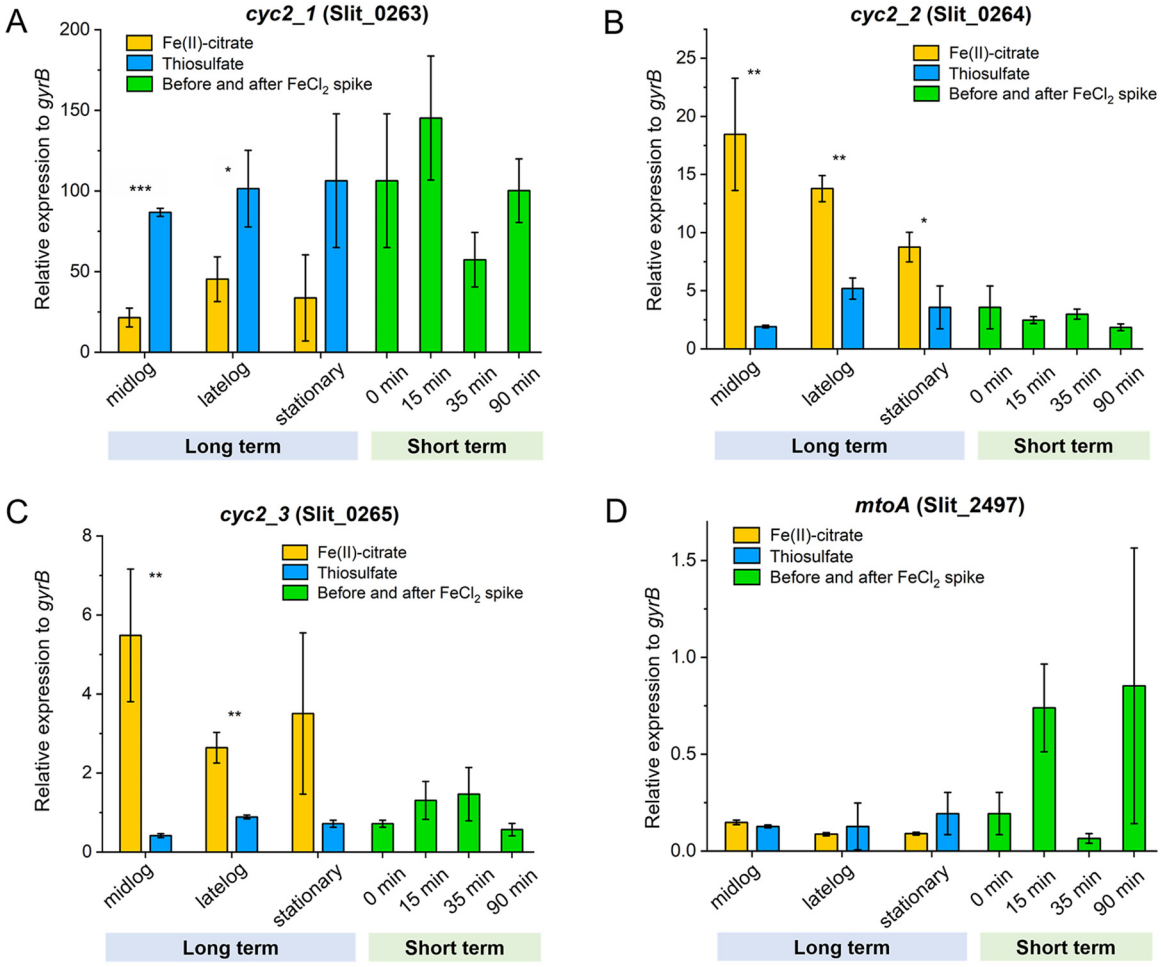

FIG 6 Relative expression by RT-qPCR of three *cyc2* genes and *mtoA* to reference *gyrB* in long-term culturing using Fe(II)-citrate and thiosulfate as the substrates and short-term $FeCl_2$ spike. (A) *cyc2_1*. (B) *cyc2_2*. (C) *cyc2_3*. (D) *mtoA*. *, $P \leq 0.05$; **, $P \leq 0.01$; ***, $P \leq 0.001$; unlabeled, not significant from Student's *t* test. For the short-term experiment, each time point was compared to 0 min, which is the stationary-phase thiosulfate-grown ES-1.

response to the short-term $FeCl_2$ spike (Fig. 6; Table S2), though the increase is not significant ($P = 0.30$). However, the DGE analysis shows a significant upregulation (>1.5-fold; $P \leq 0.01$) of *cyc2_1* at all three time points after $FeCl_2$ addition (Table S3). However, in long-term cultures, *cyc2_1* was downregulated in Fe(II)-citrate cultures compared to thiosulfate cultures. Despite this downregulation, *cyc2_1* remained one of the most highly expressed genes in both Fe(II)-citrate and thiosulfate cultures (Table S3). In contrast, the other two *cyc2* copies, *cyc2_2* and *cyc2_3*, were upregulated in long-term Fe(II)-citrate cultures compared to thiosulfate cultures (Fig. 6). Moreover, *cyc2_2* was expressed at the same level as *cyc2_1* in Fe(II)-citrate at mid-log phase, when the Fe(II) oxidation activity should be the highest, which suggests *cyc2_2* could play as important a role as *cyc2_1* in Fe(II) oxidation.

Expression of other putative Fe(II) oxidation-related genes. In addition to *cyc2* and *mtoA*, we also looked at the expression of other ES-1 genes proposed by He et al. (26) as putative Fe(II) oxidases, specifically two "porin-cytochrome *c* complex" gene clusters (PCC3), which contain a predicted beta-barrel porin, an extracellular multiheme cytochrome (MHC), a periplasmic MHC, and a hypothetical protein. ES-1 has two PCC3 gene clusters: Slit_0867 to Slit_0870, with 17 and 21 heme-binding sites (CXXCH) in the MHC genes Slit_0868 and Slit_0869, respectively, and Slit_1446 to Slit_1449, with 24 and 28 heme-binding sites in Slit_1447 and Slit_1448, respectively. While the expression level of the second PCC3 gene cluster was higher than that of the first, both

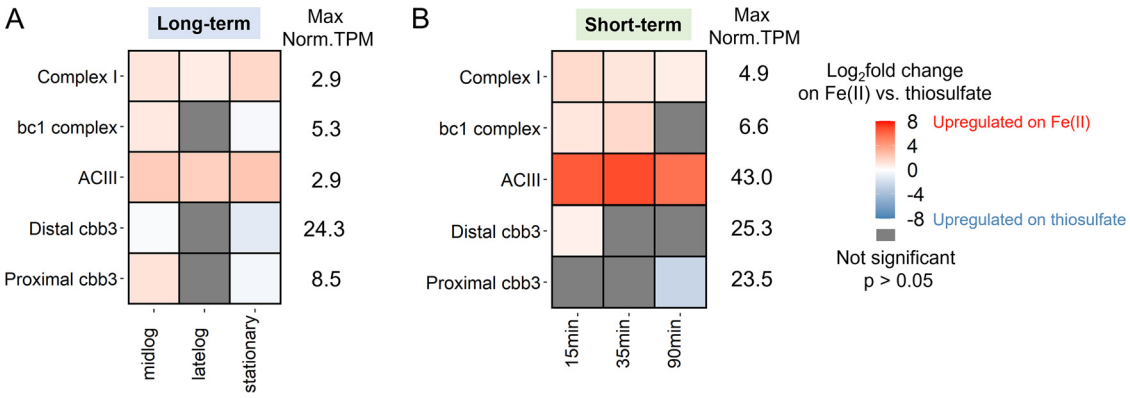

FIG 7 Differential gene expression and maximum values of constitutive normalized TPM of genes involved in "downhill" and "uphill" electron transfer in the (A) long-term and (B) short-term experiments. The $\log_2$ fold change in the heat map is the maximum $\log_2$ fold change in the gene cluster. See Tables S5 and S6 for $\log_2$ FC values and the supplemental datasheet for other genes in the cluster at https://doi.org/10.6084/m9.figshare.c.5714063.v1.

PCC3 gene clusters were downregulated in long-term Fe(II)-citrate-grown cells compared to thiosulfate-grown cells and in short-term-grown cells after $FeCl_2$ spike compared to time zero (see Table S4 in the supplemental material). Therefore, neither of the two PCC3 gene clusters appears to be involved in Fe(II) oxidation in ES-1 under our culture conditions.

We identified a novel gene cluster that was highly expressed (maximum percentile of 97.3) and Fe(II) responsive (Table S4). This gene cluster was upregulated in long-term Fe(II)-citrate culture compared to thiosulfate culture, as well as in the short-term experiment after $FeCl_2$ spike, compared to time zero. The gene cluster contains genes coding for a cytochrome *b* (Slit_1321), a hypothetical extracellular protein (Slit_1322), a monoheme cytochrome class I (Slit_1323), a diheme cytochrome *c* (Slit_1324), and a heat shock protein (Slit_1325). This gene cluster also has homologs in three other neutrophilic Fe(II) oxidizers, *Sideroxydans* sp. strain CL21, *Gallionella capsiferriformans* ES-2, and *Mariprofundus ferrooxydans* PV-1 (see Fig. S4 in the supplemental material). *Sideroxydans* sp. strain CL21 also expressed these genes highly during growth by Fe(II) oxidation (38). In all, these results are consistent with a possible role of Slit_1321 to Slit_1324 in Fe(II) oxidation.

Since Cyc2 is an outer membrane Fe(II) oxidase, electrons from Fe(II) need to be transferred to periplasmic cytochromes. We identified two highly expressed monoheme cytochrome class I genes, Slit_1353 and Slit_2042, as candidates for periplasmic electron carriers. Slit_1353 was upregulated in the long-term Fe(II)-citrate culture, whereas Slit_2042 was upregulated in the short-term culture after addition of $FeCl_2$ (Table S4). The $cyc1_{PV\text{-}1}$ homolog Slit_2657 is associated with the cbb_3-type terminal oxidase gene cluster and was upregulated in the short term after $FeCl_2$ spike (Table S4).

The expression and regulation patterns in "downhill" electron transfer to terminal oxidases. The electrons obtained from either Fe(II) or thiosulfate may be transferred "downhill" to terminal oxidases (39). In ES-1, the electrons can be passed to a cbb_3-type cytochrome oxidase to reduce oxygen (25). There are two cbb_3-type cytochrome oxidase gene clusters in the ES-1 genome, which belong to the proximal and distal cbb_3 subtrees described by Ducluzeau et al. (40) that differ in their subunit composition. The *ccoN* and *ccoO* genes from both cbb_3 gene clusters were highly expressed given the high percentile in the gene expression profile, but the constitutive normalized TPM value of distal cbb_3 is ~3-fold higher than that of the proximal cbb_3 (see Table S5 in the supplemental material). The DGE analysis shows at mid-log phase, proximal *ccoN* and *ccoO* were upregulated in Fe(II)-citrate grown culture, while the distal *ccoN* and *ccoO* were upregulated in thiosulfate culture (Fig. 7). Therefore, each cbb_3-type cytochrome oxidase may play a role in accepting electrons from different electron donors.

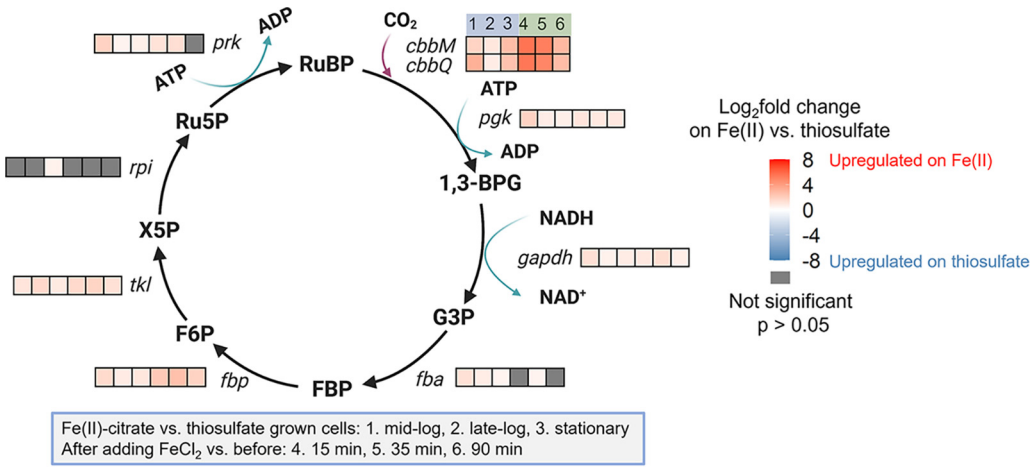

FIG 8 Differential gene expression of the genes involved in CBB cycle. Abbreviations: RuBP, ribulose 1,5-bisphosphate; 1,3 BPG, 1,3-bisphosphoglycerate; G3P, glyceraldehyde 3-phosphate; FBP, fructose 1,6-bisphosphate; F6P, fructose 6-phosphate; X5P, xylulose 5-phosphate; Ru5P, ribulose 5-phosphate.

The expression and regulation patterns in "uphill" (reverse) electron transfer. The "uphill" (reverse) electron transport pathway is used to produce reducing equivalents (NADH), which are essential in many biochemical reactions. Importantly, in autotrophic bacteria, NADH participates in CO_2 fixation to reduce the intermediates, which affects the biomass yield (41). The ES-1 genome encodes both the bc_1 complex and alternative complex III (ACIII) to potentially carry out the reverse electron transfer to complex I (41, 42). ACIII genes with high similarity have been found in many other microaerophilic FeOB, including *Gallionella capsiferriformans* ES-2 and some *Zetaproteobacteria* FeOB single amplified genomes (SAGs) (13, 21, 25). In our work, the expression level of the bc_1 complex genes (Slit_0130 to Slit_0132) showed moderate upregulation in both long-term Fe(II)-citrate culture compared to thiosulfate and after the $FeCl_2$ spike (Fig. 7; see Table S6 in the supplemental material). DGE analysis showed the ACIII gene cluster was significantly upregulated in Fe(II)-citrate at different growth phases in long-term growth, with a maximum $\log_2$ fold change (FC) of 2.36 (Table S6). After adding $FeCl_2$ to the thiosulfate culture, the ACIII gene cluster showed a sharp upregulation, with the maximum $\log_2$ FC of 6.84 (Table S6). Meanwhile, the gene cluster of NADH dehydrogenase (complex I) was also upregulated in long- and short-term response to Fe(II) substrates (Fig. 7). The upregulation of the "uphill" electron transfer chain could result in more production of NADH during Fe(II) oxidation, to be further used in various biochemical reactions.

Regulation patterns of CO_2 fixation. CO_2 fixation is an important NADH sink (43, 44). In ES-1, CO_2 fixation is achieved through Calvin-Benson-Bassham (CBB) cycle, in which RuBisCO proteins are the key enzymes (25). ES-1 encodes two types of RuBisCO: form I *cbbLS* (Slit_0985 to Slit_0986) and form II *cbbMQ* (Slit_0022 to Slit_0023). The maximum normalized TPM of form II *cbbMQ* was over 100-fold higher than the form I *cbbLS*, and *cbbMQ* expression was higher than *cbbLS* expression under all conditions tested, which were all microaerobic, suggesting form II *cbbMQ* might play a major role in ES-1 CO_2 fixation under low O_2 concentrations. Form II enzymes, which have a higher affinity for O_2, can function in low-O_2 and high-CO_2 environments (45), such as the preferred geochemical niches of microaerophilic FeOB like ES-1. RuBisCO (*cbbMQ*) and most of the other genes involved in the CBB cycle were upregulated in long- and short-term responses to Fe(II) (Fig. 8). Moreover, the short-term response showed a sharp upregulation of *cbbMQ*, with a $\log_2$ FC greater than 5, which is consistent with the ACIII regulation pattern.

Phage genes. ES-1 has two clusters of prophage genes, and these genes are among the most responsive to the change in substrates. The first phage cluster (Slit_0188 to Slit_0249; 39.7 kb) belongs to a Mu-like prophage family, and a subset of these genes

have homology to a prophage in the marine microaerophilic FeOB *Mariprofundus ferrooxydans* PV-1 (25). The second phage gene cluster (Slit_1888 to Slit_1969; 54.3 kb) does not have homologs in PV-1, and the majority of the genes have hypothetical or unknown function. The DGE analysis showed the first phage cluster is Fe(II) responsive [upregulated in Fe(II)-citrate culture], with a maximum $\log_2$ FC of 7.90, whereas the second phage cluster is thiosulfate responsive (upregulated in thiosulfate culture). These data do not illuminate whether these gene expression trends are due to induction of the prophage within some fraction of the ES-1 population into an active lytic cycle or whether they are the result of lysogenic conversion (i.e., host expression of integrated prophage genes). However, the result does suggest that the phage gene clusters may represent auxiliary metabolic genes (46) that could play a role in ES-1 Fe(II) and thiosulfate oxidation and/or that the phage activation itself may be responsive to the availability and oxidative metabolism of these compounds.

DISCUSSION

Sideroxydans lithotrophicus ES-1 was isolated as an Fe(II) oxidizer and was later discovered to also grow by thiosulfate oxidation (24, 25). This makes it unusual among the *Gallionellaceae*, in which most other isolates are obligate Fe(II) oxidizers (*Gallionella*, *Ferriphaselus*, and *Ferrigenium* spp.). Previous studies have shown *Sideroxydans* isolates are abundant in environments with both Fe(II) and reduced S species (17, 21–23). Our data show ES-1 has higher yields on thiosulfate (Fig. 1A; Fig. S2) and can grow simultaneously on Fe(II) and thiosulfate (Fig. 1A to C). Our growth studies show that the addition of thiosulfate can boost *Sideroxydans* growth in the presence or absence of Fe(II), giving it an advantage over obligate FeOB in niches where both Fe and S are available.

Because different pathways are used to oxidize Fe(II) versus thiosulfate, cells might conserve energy by expressing only the genes necessary for the available or desired electron donor(s). We performed experiments in which we switched the substrate and observed a lag in substrate consumption when switching from Fe(II) to thiosulfate (Fig. 1C), but no lag when switching from thiosulfate to Fe(II) (Fig. 1D). This is consistent with the expression patterns of Fe(II)- and thiosulfate-oxidizing genes. There was relatively high expression of Fe(II) oxidase gene *cyc2_1* during the thiosulfate-only growth (Fig. 5 and 6), whereas S oxidation genes were expressed at low levels during Fe(II) oxidation and significantly upregulated on thiosulfate (Fig. 4). This contrast suggests that *Sideroxydans* maintains readiness to oxidize Fe(II), while thiosulfate oxidation serves as a secondary, supporting metabolism in either the presence or absence of Fe(II). In this case, despite the ability to oxidize a sulfur compound, the *Sideroxydans* niche appears to be primarily in Fe(II) oxidation, consistent with its known environmental distribution.

The differential gene expression on Fe(II) versus thiosulfate gives us insight into the genes that may be specific to each metabolism. ES-1 upregulated *dsr* and *sox* genes on thiosulfate, despite the expectation that *tsd* would be upregulated, since thiosulfate is incompletely oxidized to tetrathionate. The Dsr and Sox pathways are not known to produce tetrathionate, and ES-1 has not yet been shown to oxidize sulfide, so the specific roles of the ES-1 *dsr* and *sox* genes require further investigation, and the genes might prove to have different functions in ES-1 compared to other sulfur-oxidizing microbes. Still, the *dsr* and *sox* gene expression does correspond to thiosulfate oxidation activity in ES-1.

The ES-1 genome encodes several proposed Fe(II) oxidation pathways, including those involving Cyc2, Mto, and PCC3. Overall, the *cyc2* expression levels were much higher than those of *mtoA* or PCC3 in the presence of Fe(II), and *cyc2_1* was among the top expressed genes (>99th percentile; Tables S3 and S4), suggesting the importance of *cyc2* in Fe(II) oxidation. The presence of three *cyc2* genes further suggests the utility since multiple copies might enable ES-1 to increase its Fe(II) oxidation capacity or efficiency (47–49). The three *cyc2* genes had different responses to Fe(II) in the short- and

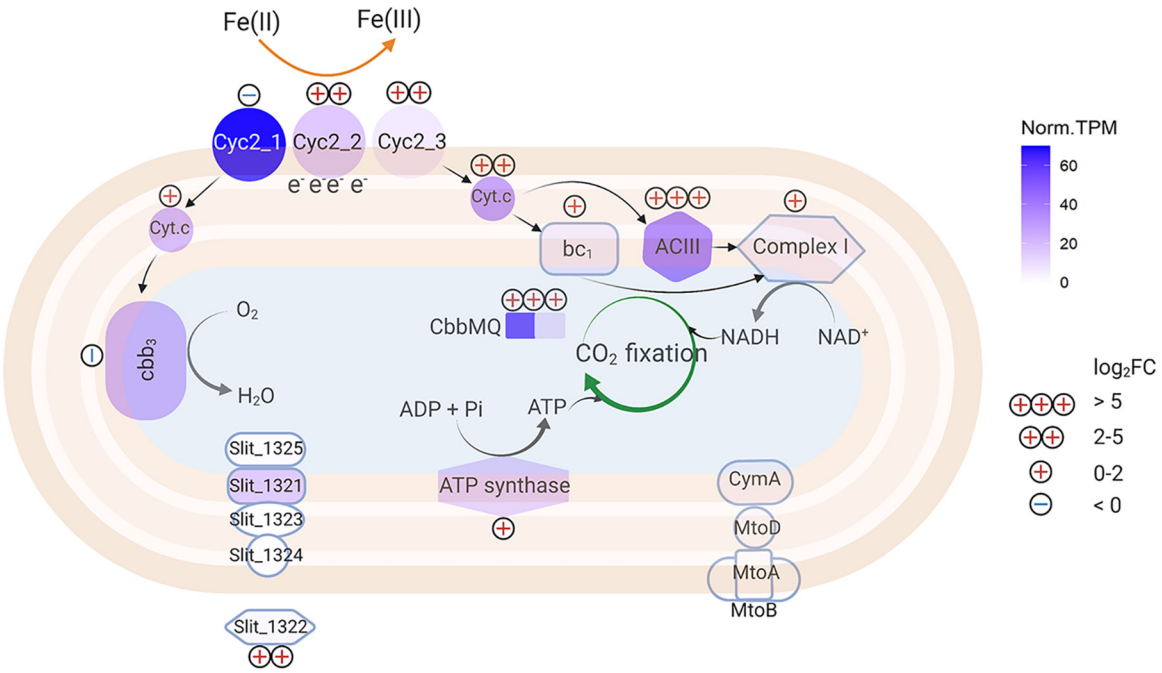

FIG 9 Updated Fe(II) oxidation pathway in ES-1. Norm. TPM represents the maximum normalized TPM using constitutively expressed genes; log_2FC represents the maximum log_2 fold change in Fe(II) culture compared to thiosulfate culture (including both long-term and short-term data). The protein location of Slit_1321 to Slit_1325 was predicted using PSORTb version 3.0.2 (68). The figure was created using Biorender.com.

long-term experiments, suggesting that each gene plays a distinct role. The first copy, *cyc2_1*, increased expression on Fe(II) in the short-term experiment, but overall was highly expressed under all conditions, including the thiosulfate-grown culture. This continuous expression may imply regulation at the protein expression level. However, thiosulfate-grown cells were able to immediately oxidize Fe(II) (Fig. 1D), suggesting that Cyc2 is indeed expressed, possibly to maintain "readiness" for Fe(II) oxidation. Addition of Fe(II) triggers the expression of *cyc2_2* and *cyc2_3* (Fig. 6; Tables S2 and S3), which would allow for more efficient transcription and translation when Fe(II) levels are high. In all, the *cyc2* expression levels and patterns support the model of a Cyc2-based Fe(II) oxidation pathway.

For neutrophilic FeOB like ES-1, the Cyc2 Fe(II) oxidation pathway was originally deduced from comparative genomics, and recent work has verified the Fe(II)-oxidizing function of $Cyc2_{PV-1}$ (29), a relatively close homolog of $Cyc2_{ES-1}$. Apart from Cyc2, the rest of the pathway has not been tested in neutrophilic FeOB isolates (25). Here, we constrained and updated the model based on gene expression levels and differential expression (Fig. 9). We identified likely periplasmic cytochromes that could act as electron carriers to transfer electrons from an outer membrane Fe(II) oxidase to the "uphill" (Slit_1353 and Slit_2042) and "downhill" (Slit_2657) electron transfer pathways (Fig. 9; Table S4). Both long-term and short-term data showed upregulation of RET and CO_2 fixation-related genes in the presence of Fe(II) (Fig. 7 and 8), which suggests electrons from Fe(II) tend to pass through RET to CO_2. Notably, genes for ACIII and RuBisCO were massively upregulated after the Fe(II) pulse. ACIII gene clusters in Fe(II)-oxidizing *Betaproteobacteria* and *Zetaproteobacteria* have a high degree of similarity, leading to a hypothesized role in Fe(II) oxidation, though the actual function remained unclear (26, 50–52). Our result suggests ACIII mainly participates in RET to provide reducing equivalents for the CO_2 fixation. In this model, CO_2 is an important electron sink to maintain redox balance, similar to photoautotrophic FeOB (43, 44).

In all, our results provide a clearer view of *Sideroxydans lithotrophicus* ES-1's physiology and gene responses to Fe(II) and thiosulfate oxidation, which may be applied

to understanding environmental Fe(II) oxidation. Detection of microbial/biotic Fe(II) oxidation in the environment has historically been difficult since biotically and abiotically formed Fe(III) oxides are not necessarily distinct by either mineralogy or isotope composition (53). There is now the potential to use the expression of Fe(II) oxidation genes to signal environmental Fe(II) oxidation if gene expression can be linked to activity. The most obvious candidates for Fe(II) oxidation gene markers are Fe(II) oxidase genes. In the case of ES-1, this is *cyc2*, and in fact, *cyc2* homologs are common across the Fe(II)-oxidizing *Gallionellaceae* and *Zetaproteobacteria* (26, 50, 52, 54). Furthermore, Cyc2 from multiple organisms, including the zetaproteobacterium *Mariprofundus ferrooxydans*, has been shown to oxidize Fe(II) (27, 29, 55). The *cyc2* genes are highly expressed in Fe(II)-oxidizing environments, as shown by metatranscriptomic studies on marine *Zetaproteobacteria* iron mats (52) and an Fe-rich aquifer dominated by *Gallionellaceae* (of which *Sideroxydans lithotrophicus* ES-1 is a member) (7). Although microbial activity and gene expression can be equated with Fe(II) oxidation activity in obligate FeOB, like many *Zetaproteobacteria*, our work revealed a more complicated picture in a facultative FeOB, which also expressed *cyc2* under non-Fe(II)-oxidizing conditions. In environments with facultative FeOB, *cyc2* or another Fe(II) oxidase gene may not be sufficient for monitoring Fe(II) oxidation activity. Instead, we can monitor gene expression for the full Fe(II) oxidation pathway, including forward and reverse electron transport (Fig. 9). Our work suggests that the full pathway can be used as a multigene indicator of Fe(II) oxidation activity, and coupled monitoring of C fixation genes can further signal Fe(II) oxidation-driven C fixation, thus showing interconnected Fe-C biogeochemical cycling in the environment.

MATERIALS AND METHODS

Cell cultivation. *Sideroxydans lithotrophicus* ES-1 was grown in 80 ml modified Wolfe's minimal medium (MWMM), which contains 1 g/liter NH_4Cl, 0.5 g/liter $MgSO_4 \cdot 7H_2O$, 0.2 g/liter $CaCl_2$, and 0.05 g/liter K_2HPO_4. The MWMM was buffered with 20 mM 2-(*N*-morpholino)ethanesulfonic acid (MES) and adjusted to pH 6.0. The liquid medium was deoxygenated by purging with nitrogen gas. Medium was supplemented with Wolfe's vitamin and trace mineral solution (ATCC, 2672) in a 1:1,000 ratio after autoclaving (56). The headspace was maintained at 2% O_2, 20% CO_2, and 78% N_2 by flushing daily. Culturing on Fe(II)-citrate was sustained with a one-time addition of sodium citrate to a final medium concentration of 5 mM and a daily addition of $FeCl_2$ stock solution. Cell cultivation on thiosulfate was performed by a one-time addition of sodium thiosulfate. The substrate concentration was varied (Fe, 100 to 750 μM/day; thiosulfate, 0.5 to 10 mM) to optimize growth (Fig. S2). Culture bottles were incubated without shaking in the dark at room temperature. The cell number was determined by counting Syto13-stained cells under fluorescence microscopy using a Hausser counting chamber.

ES-1 substrate consumption experiment. Ferrous chloride ($FeCl_2$)-grown cells were inoculated into MWMM with both $FeCl_2$ and thiosulfate, $FeCl_2$ only, or thiosulfate only. The uninoculated medium with both $FeCl_2$ and thiosulfate was used as the abiotic control. All treatments were performed in triplicate. Substrates ($FeCl_2$ and sodium thiosulfate) were amended daily to maintain a concentration of 500 μM. The headspace was flushed with gas mix (O_2-CO_2-N_2 at 2:20:78) every day. The cell number was recorded every 2 days by direct cell counting. Fe(II) and thiosulfate concentrations were determined every day before and after the substrate supplement. The levels of biotic Fe(II) and thiosulfate consumption per day were calculated by subtracting the substrate loss in the uninoculated control from the substrate loss in the live culture. The electron uptake rate was calculated by the following equation: electron uptake rate = (substrate concn_t − substrate concn_0)/(cell no. per L × t).

Chemical analysis. The Fe(II) concentration was determined by spectrophotometric ferrozine assay (57, 58). To ensure oxygen was maintained between 20 and 30 μM, the oxygen concentration in the cultures was measured using a Firesting oxygen meter coupled with a fiber optic probe and with a sensor spot inside the serum bottle (Pyro Science). The oxygen consumption in cultures fed 500 μM (per day) Fe(II)-citrate culture or 10 mM thiosulfate culture is shown in Fig. S5 in the supplemental material. The thiosulfate concentration was determined by mixing samples with the same volume of 1 mM iodine solution, then the absorbance at 350 nm was measured (59). The sulfur speciation was identified using high-performance liquid chromatography (HPLC) (69, 70). Samples were separated on an Alltech organic acid 5-μm column (150 by 4.6 mm) eluted with 25 mM potassium phosphate buffer at 1 mL/min (pH 2.5) on a Shimadzu Class-10VP HPLC device. Detection was at 210 nm. Thiosulfate and tetrathionate standards were prepared and diluted in growth medium to generate a standard curve and calibrate the retention time for each compound.

Transcriptome experiment culturing and sampling. Transcriptome analysis was used to investigate the genes expressed during Fe(II) and thiosulfate oxidation. To obtain sufficient biomass for RNA extraction, the culture was scaled up to 250 mL of medium in 500-mL glass culture bottles. We investigated both long-term and short-term responses of ES-1 to different Fe(II) substrates. To investigate the

long-term response, we cultivated ES-1 using Fe(II)-citrate or thiosulfate as described above, then sampled different growth phases. Fe(II)-citrate grown cells were sampled on day 2 (mid-log), day 5 (late-log), and day 7 (stationary). Samples from thiosulfate-grown cells were taken on day 3 (mid-log), day 7 (late-log), and day 10 (stationary). Since the Fe(II)-citrate-grown cultures had lower cell density, three culture bottles were combined (750 mL total) for each sample. The thiosulfate-grown cultures had higher cell density; therefore, only one bottle (250 mL) of culture was harvested for each sample. To investigate short-term, rapid gene expression responses to Fe(II), we spiked $FeCl_2$ stock solution into stationary-phase thiosulfate-grown ES-1 culture to a final concentration of 100 μM, and the killed-cell control was created by adding sodium azide into the culture to a final concentration of 5 mM. Samples were taken at 0, 15, 35, 60, and 90 min for the ferrozine assay to track the Fe(II) oxidation kinetics. Meanwhile, culture bottles were sacrificed for RNA extraction at the beginning (15 min), middle (35 min), and end of the Fe(II) oxidation (90 min). For each time point in the long-term and short-term experiment, samples were collected in biological triplicate. To protect cellular RNA from degradation, 1/10 volume of stop solution (buffer-saturated phenol–absolute ethanol at 1:9 [vol/vol]) was added to the culture (60), and cells were harvested by collecting the culture on a 0.22-μm-pore membrane (Millipore, GTTP). The filter membranes with cells were then cut into small pieces and stored at −80°C until RNA extraction.

RNA extraction. The cells were lysed by high-speed vortexing for 2 min using lysing matrix E tubes (MP Biomedical) in buffer RLT (Qiagen) amended with 1% 2-mercaptoethanol. The lysate was centrifuged at 4,000 $\times$ *g* for 10 min at 4°C. The supernatant was collected and extracted using the Qiagen Micro RNeasy kit following the instructions provided by the manufacturer. The samples were then treated with the Turbo DNase kit (Invitrogen) to remove genomic DNA. The rRNA in the total RNA samples was depleted using MICROBExpress bacterial mRNA purification kit (Invitrogen). The rRNA-depleted samples were further purified and concentrated using Zymo RNA Clean and Concentrator kit. The RNA concentration was quantified on a Qubit fluorometer using the Qubit RNA HS assay kit (Invitrogen). The RNA quality was determined on the Agilent fragment analyzer at the University of Delaware DNA Sequencing & Genotyping Center.

RT-qPCR. Total RNA (20 ng) was used as the template to synthesize cDNA using the Maxima First Strand cDNA synthesis kit (Thermo Scientific). Gene expression of three *cyc2* genes (Slit_0263, Slit_0264, and Slit_0265) and *mtoA* (Slit_2497) was quantified using RT-qPCR with *gyrB* (Slit_0003) as a reference gene. Primers for the target genes were designed (sequences in Table S7 in the supplemental material). Quantabio SYBR green supermix and the Bio-Rad CFX96 real-time PCR system were used to perform the quantification assays. Standard curves were generated using cloned plasmids containing the target DNA fragments with the concentration range from 500 ag/μL to 50 pg/μL. The target genes were amplified using the following program: 95°C 5 min, followed by 40 cycles of 95°C for 15 s, then the indicated annealing temperature of each primer set for 45 s (Table S7), then 72°C for 30 s, followed by a melt curve analysis from 55 to 65°C. The gene copy numbers were calculated using the quantification cycle (C_q) values and the standard curves for each gene. Each biological replicate was run in two technical replicates. The *P* values of RT-qPCR were generated from Student's *t* test, and the cutoff of significant change is $P \leq 0.05$.

RNA sequencing and analysis. The library preparation and sequencing were performed at the University of Delaware DNA Sequencing & Genotyping Center. The Nextflex Rapid Directional RNA-Seq kit was used for library preparation. Sequencing was performed on Illumina NextSeq 550 sequencing system with a read length of 1 $\times$ 76 bp. The transcriptomic reads were quality controlled using FastQC v0.11.9 (Babraham Bioinformatics). The low-quality reads were trimmed using Trim Galore! v0.6.4 (61) with a cutoff Q score of 28. After trimming, the average number of reads per sample was 19.6 M. Then the trimmed reads were mapped to the ES-1 genome (GenBank accession no. NC_013959) using bowtie2 v2.3.5.1 (62). The overall average alignment rate among all the samples was 98.3%. Next, samtools v1.9 was used to sort and index the aligned file (63). The sorted .bam files were counted using Htseq-count (64) with an annotated ES-1 gff file. To evaluate the gene expression level, we first normalized the read counts to transcripts per million (TPM), which accounts for both gene length and library size, then TPM values were further normalized by dividing by the average TPM values of six constitutively expressed genes (*gyrB*, *gyrA*, *adk*, *rho*, *era*, and *gmk*) (35). The percentile of gene expression was calculated based on the constitutive normalized TPM. The output counting file was used to analyze the differential gene expression using Bioconductor DESeq2 v1.26.0 (65), and *P* values were generated from the Wald test and then false-discovery rate (FDR) adjusted using the Benjamini-Hochberg (BH) correction (66). For the long-term experiment, simple pairwise comparison was performed between Fe(II)-citrate- and thiosulfate-grown cells at each different growth phase, with thiosulfate-grown cells as the control. For the short-term experiment, the control was time zero (thiosulfate-grown cells in stationary phase), and other time points after Fe(II) addition were pairwise compared with time zero. Genes with zero counts were removed from the DGE analysis. Genes with *P* values of ≤0.05 were considered differentially expressed. Heat maps were made in R using ggplot2 (67). A master spreadsheet with raw counts, constitutive normalized TPM values and DGE analysis results is provided as a supplemental file at https://doi.org/10.6084/m9.figshare.c.5714063.v1.

Data availability. Transcriptomic data were uploaded to NCBI BioProject no. PRJNA753090. Raw RNA-Seq reads can be accessed through Sequence Read Archive (SRA) accession no. SRP331695.

SUPPLEMENTAL MATERIAL

Supplemental material is available online only.

SUPPLEMENTAL FILE 1, PDF file, 0.8 MB.

ACKNOWLEDGMENTS

This work is funded by NASA Exobiology (80NSSC18K1292 to C.S.C.), NSF Geobiology and Low Temperature Geochemistry (EAR-1833525 to C.S.C. and S.W.P.), ONR grant N00014-17-1-2640 (to C.S.C.), and the Joanne Daiber Fellowship (to N.Z.). We acknowledge the University of Delaware DNA Sequencing Center for RNA sequencing and Delaware INBRE for transcriptomic data processing using Biomix (NIH P20 GM103446).

We thank Thomas Hanson for help in characterizing thiosulfate oxidation products and David Emerson for comments on an early version of the manuscript.

We declare no conflict of interest.

REFERENCES

1. Achberger AM, Christner BC, Michaud AB, Priscu JC, Skidmore ML, Vick-Majors TJ. 2016. Microbial community structure of subglacial Lake Whillans, West Antarctica. Front Microbiol 7:1457. https://doi.org/10.3389/fmicb.2016.01457.
2. Dubinina GA, Sorokina AY. 2014. Neutrophilic lithotrophic iron-oxidizing prokaryotes and their role in the biogeochemical processes of the iron cycle. Microbiology 83:1–14. https://doi.org/10.1134/S0026261714020052.
3. Chan CS, McAllister SM, Leavitt AH, Glazer BT, Krepski ST, Emerson D. 2016. The architecture of iron microbial mats reflects the adaptation of chemolithotrophic iron oxidation in freshwater and marine environments. Front Microbiol 7:796. https://doi.org/10.3389/fmicb.2016.00796.
4. Nakagawa K, Murase J, Asakawa S, Watanabe T. 2020. Involvement of microaerophilic iron-oxidizing bacteria in the iron-oxidizing process at the surface layer of flooded paddy field soil. J Soils Sediments 20:4034–4041. https://doi.org/10.1007/s11368-020-02717-w.
5. Maisch M, Lueder U, Laufer K, Scholze C, Kappler A, Schmidt C. 2019. Contribution of microaerophilic iron(II)-oxidizers to iron(III) mineral formation. Environ Sci Technol 53:8197–8204. https://doi.org/10.1021/acs.est.9b01531.
6. Druschel GK, Emerson D, Sutka R, Suchecki P, Luther GW. 2008. Low-oxygen and chemical kinetic constraints on the geochemical niche of neutrophilic iron(II) oxidizing microorganisms. Geochim Cosmochim Acta 72:3358–3370. https://doi.org/10.1016/j.gca.2008.04.035.
7. Jewell TNM, Karaoz U, Brodie EL, Williams KH, Beller HR. 2016. Metatranscriptomic evidence of pervasive and diverse chemolithoautotrophy relevant to C, S, N and Fe cycling in a shallow alluvial aquifer. ISME J 10:2106–2117. https://doi.org/10.1038/ismej.2016.25.
8. Sowers TD, Holden KL, Coward EK, Sparks DL. 2019. Dissolved organic matter sorption and molecular fractionation by naturally occurring bacteriogenic iron (oxyhydr)oxides. Environ Sci Technol 53:4295–4304. https://doi.org/10.1021/acs.est.9b00540.
9. Emerson D, Fleming EJ, McBeth JM. 2010. Iron-oxidizing bacteria: an environmental and genomic perspective. Annu Rev Microbiol 64:561–583. https://doi.org/10.1146/annurev.micro.112408.134208.
10. McAllister SM, Moore RM, Gartman A, Luther GW, Emerson D, Chan CS. 2019. The Fe(II)-oxidizing Zetaproteobacteria: historical, ecological and genomic perspectives. FEMS Microbiol Ecol 95:fiz015. https://doi.org/10.1093/femsec/fiz015.
11. Ankrah NYD, May AL, Middleton JL, Jones DR, Hadden MK, Gooding JR, LeCleir GR, Wilhelm SW, Campagna SR, Buchan A. 2014. Phage infection of an environmentally relevant marine bacterium alters host metabolism and lysate composition. ISME J 8:1089–1100. https://doi.org/10.1038/ismej.2013.216.
12. Adhikari D, Zhao Q, Das K, Mejia J, Huang R, Wang X, Poulson SR, Tang Y, Roden EE, Yang Y. 2017. Dynamics of ferrihydrite-bound organic carbon during microbial Fe reduction. Geochim Cosmochim Acta 212:221–233. https://doi.org/10.1016/j.gca.2017.06.017.
13. Wu R, Wang C, Shen J, Zhao F. 2015. Role for biosynthetic CdS quantum dots in extracellular electron transfer of Saccharomyces cerevisiae. Process Biochem 50:2061–2065. https://doi.org/10.1016/j.procbio.2015.10.005.
14. Arkin AP, Stevens RL, Cottingham RW, Maslov S, Henry CS, Dehal P, Ware D, Perez F, Harris NL, Canon S, Sneddon MW, Henderson ML, Riehl WJ, Gunter D, Murphy-Olson D, Chan S, Kamimura RT, Brettin TS, Meyer F, Chivian D, Weston DJ, Glass EM, Davison BH, Kumari S, Allen BH, Baumohl J, Best AA, Bowen B, Brenner SE, Bun CC, Chandonia J-M, Chia J-M, Colasanti R, Conrad N, Davis JJ, DeJongh M, Devoid S, Dietrich E, Drake MM, Dubchak I, Edirisinghe JN, Fang G, Faria JP, Frybarger PM, Gerlach W, Gerstein M, Gurtowski J, Haun HL, He F, Jain R, et al. 2016. The DOE Systems Biology Knowledgebase (KBase). bioRxiv 96354. https://www.biorxiv.org/content/10.1101/096354v1.
15. Chinni S, Anderson CR, Ulrich K-U, Giammar DE, Tebo BM. 2008. Indirect UO_2 oxidation by Mn(II)-oxidizing spores of Bacillus sp. strain SG-1 and the effect of U and Mn concentrations. Environ Sci Technol 42:8709–8714. https://doi.org/10.1021/es801388p.
16. Lüdecke C, Reiche M, Eusterhues K, Nietzsche S, Küsel K. 2010. Acid-tolerant microaerophilic Fe(II)-oxidizing bacteria promote Fe(III)-accumulation in a fen. Environ Microbiol 12:2814–2825.
17. Herrmann M, Opitz S, Harzer R, Totsche K, Küsel K. 2017. Attached and suspended denitrifier communities in pristine limestone aquifers harbor high fractions of potential autotrophs oxidizing reduced iron and sulfur compounds. Microb Ecol 74:264–277. https://doi.org/10.1007/s00248-017-0950-x.
18. Boyd ES, Hamilton TL, Havig JR, Skidmore ML, Shock EL. 2014. Chemolithotrophic primary production in a subglacial ecosystem. Appl Environ Microbiol 80:6146–6153. https://doi.org/10.1128/AEM.01956-14.
19. Wang J, Sickinger M, Ciobota V, Herrmann M, Rasch H, Rösch P, Popp J, Küsel K. 2014. Revealing the microbial community structure of clogging materials in dewatering wells differing in physico-chemical parameters in an open-cast mining area. Water Res 63:222–233. https://doi.org/10.1016/j.watres.2014.06.021.
20. Fabisch M, Beulig F, Akob DM, Küsel K. 2013. Surprising abundance of Gallionella-related iron oxidizers in creek sediments at pH 4.4 or at high heavy metal concentrations. Front Microbiol 4:390. https://doi.org/10.3389/fmicb.2013.00390.
21. Arce-Rodríguez A, Puente-Sánchez F, Avendaño R, Martínez-Cruz M, de Moor JM, Pieper DH, Chavarría M. 2019. Thermoplasmatales and sulfur-oxidizing bacteria dominate the microbial community at the surface water of a CO_2-rich hydrothermal spring located in Tenorio Volcano National Park, Costa Rica. Extremophiles 23:177–187. https://doi.org/10.1007/s00792-018-01072-6.
22. Jin L, Lee CS, Ahn CY, Lee HG, Lee S, Shin HH, Lim D, Oh HM. 2017. Abundant iron and sulfur oxidizers in the stratified sediment of a eutrophic freshwater reservoir with annual cyanobacterial blooms. Sci Rep 7:43814. https://doi.org/10.1038/srep43814.
23. Chi H, Yang L, Yang W, Li Y, Chen Z, Huang L, Chao Y, Qiu R, Wang S. 2018. Variation of the bacterial community in the rhizoplane iron plaque of the wetland plant Typha latifolia. I J Environ Res Public Health 15:2610. https://doi.org/10.3390/ijerph15122610.
24. Emerson D, Moyer C. 1997. Isolation and characterization of novel iron-oxidizing bacteria that grow at circumneutral pH. Appl Environ Microbiol 63:4784–4792. https://doi.org/10.1128/aem.63.12.4784-4792.1997.
25. Emerson D, Field EK, Chertkov O, Davenport KW, Goodwin L, Munk C, Nolan M, Woyke T. 2013. Comparative genomics of freshwater Fe-oxidizing bacteria: implications for physiology, ecology, and systematics. Front Microbiol 4:254. https://doi.org/10.3389/fmicb.2013.00254.
26. He S, Barco RA, Emerson D, Roden EE. 2017. Comparative genomic analysis of neutrophilic iron(II) oxidizer genomes for candidate genes in extracellular electron transfer. Front Microbiol 8:1584. https://doi.org/10.3389/fmicb.2017.01584.
27. Castelle C, Guiral M, Malarte G, Ledgham F, Leroy G, Brugna M, Giudici-Orticoni MT. 2008. A new iron-oxidizing/O_2-reducing supercomplex spanning both inner and outer membranes, isolated from the extreme acidophile Acidithiobacillus ferrooxidans. J Biol Chem 283:25803–25811. https://doi.org/10.1074/jbc.M802496200.

28. Singer E, Emerson D, Webb EA, Barco RA, Kuenen JG, Nelson WC, Chan CS, Comolli LR, Ferriera S, Johnson J, Heidelberg JF, Edwards KJ. 2011. Mariprofundus ferrooxydans PV-1 the first genome of a marine Fe(II) oxidizing zetaproteobacterium. PLoS One 6:e25386. https://doi.org/10.1371/journal.pone.0025386.
29. Keffer JL, McAllister SM, Garber AI, Hallahan BJ, Sutherland MC, Rozovsky S, Chan CS. 2021. Iron oxidation by a fused cytochrome-porin common to diverse iron-oxidizing bacteria. mBio 12:e01074-21. https://doi.org/10.1128/mBio.01074-21.
30. Liu J, Wang Z, Belchik SM, Edwards MJ, Liu C, Kennedy DW, Merkley ED, Lipton MS, Butt JN, Richardson DJ, Zachara JM, Fredrickson JK, Rosso KM, Shi L. 2012. Identification and characterization of MtoA: a decaheme c-type cytochrome of the neutrophilic Fe(II)-oxidizing bacterium Sideroxydans lithotrophicus ES-1. Front Microbiol 3:37.
31. Chan CS, Fakra SC, Emerson D, Fleming EJ, Edwards KJ. 2011. Lithotrophic iron-oxidizing bacteria produce organic stalks to control mineral growth: implications for biosignature formation. ISME J 5:717–727. https://doi.org/10.1038/ismej.2010.173.
32. Shi L, Dong H, Reguera G, Beyenal H, Lu A, Liu J, Yu H-Q, Fredrickson JK. 2016. Extracellular electron transfer mechanisms between microorganisms and minerals. Nat Rev Microbiol 14:651–662. https://doi.org/10.1038/nrmicro.2016.93.
33. Chan CS, Fakra SC, Edwards DC, Emerson D, Banfield JF. 2009. Iron oxyhydroxide mineralization on microbial extracellular polysaccharides. Geochim Cosmochim Acta 73:3807–3818. https://doi.org/10.1016/j.gca.2009.02.036.
34. Zhou N, Luther GW, Chan CS. 2021. Ligand effects on biotic and abiotic Fe (II) oxidation by the microaerophile Sideroxydans lithotrophicus. Environ Sci Technol 55:9362–9371. https://doi.org/10.1021/acs.est.1c00497.
35. Rocha DJP, Santos CS, Pacheco LGC. 2015. Bacterial reference genes for gene expression studies by RT-qPCR: survey and analysis. Antonie Van Leeuwenhoek 108:685–693. https://doi.org/10.1007/s10482-015-0524-1.
36. Friedrich CG, Bardischewsky F, Rother D, Quentmeier A, Fischer J. 2005. Prokaryotic sulfur oxidation. Curr Opin Microbiol 8:253–259. https://doi.org/10.1016/j.mib.2005.04.005.
37. Kurth JM, Brito JA, Reuter J, Flegler A, Koch T, Franke T, Klein EM, Rowe SF, Butt JN, Denkmann K, Pereira IAC, Archer M, Dahl C. 2016. Electron accepting units of the diheme cytochrome c TsdA, a bifunctional thiosulfate dehydrogenase/tetrathionate reductase. J Biol Chem 291:24804–24818. https://doi.org/10.1074/jbc.M116.753863.
38. Cooper RE, Wegner C-E, Kügler S, Poulin RX, Ueberschaar N, Wurlitzer JD, Stettin D, Wichard T, Pohnert G, Küsel K. 2020. Iron is not everything: unexpected complex metabolic responses between iron-cycling microorganisms. ISME J 14:2675–2690. https://doi.org/10.1038/s41396-020-0718-z.
39. Brasseur G, Levican G, Bonnefoy V, Holmes D, Jedlicki E, Lemesle-Meunier D. 2004. Apparent redundancy of electron transfer pathways via bc1 complexes and terminal oxidases in the extremophilic chemolithoautotrophic Acidithiobacillus ferrooxidans. Biochim Biophys Acta 1656:114–126. https://doi.org/10.1016/j.bbabio.2004.02.008.
40. Ducluzeau AL, Ouchane S, Nitschke W. 2008. The cbb3 oxidases are an ancient innovation of the domain bacteria. Mol Biol Evol 25:1158–1166. https://doi.org/10.1093/molbev/msn062.
41. Elbehti A, Brasseur G, Lemesle-Meunier D. 2000. First evidence for existence of an uphill electron transfer through the bc1 and NADH-Q oxidoreductase complexes of the acidophilic obligate chemolithotrophic ferrous ion-oxidizing bacterium Thiobacillus ferrooxidans. J Bacteriol 182:3602–3606. https://doi.org/10.1128/JB.182.12.3602-3606.2000.
42. Refojo PN, Teixeira M, Pereira MM. 2012. The alternative complex III: properties and possible mechanisms for electron transfer and energy conservation. Biochim Biophys Acta 1817:1852–1859. https://doi.org/10.1016/j.bbabio.2012.05.003.
43. Guzman MS, Rengasamy K, Binkley MM, Jones C, Ranaivoarisoa TO, Singh R, Fike DA, Meacham JM, Bose A. 2019. Phototrophic extracellular electron uptake is linked to carbon dioxide fixation in the bacterium Rhodopseudomonas palustris. Nat Commun 10:1355. https://doi.org/10.1038/s41467-019-09377-6.
44. Bose A, Gardel EJ, Vidoudez C, Parra EA, Girguis PR. 2014. Electron uptake by iron-oxidizing phototrophic bacteria. Nat Commun 5:3391. https://doi.org/10.1038/ncomms4391.
45. Badger MR, Bek EJ. 2008. Multiple Rubisco forms in proteobacteria: their functional significance in relation to CO_2 acquisition by the CBB cycle. J Exp Bot 59:1525–1541. https://doi.org/10.1093/jxb/erm297.
46. Breitbart M, Thompson L, Suttle C, Sullivan M. 2007. Exploring the vast diversity of marine viruses. Oceanography 20:135–139. https://doi.org/10.5670/oceanog.2007.58.
47. Nowak MA, Boerlijst MC, Cooke J, Smith JM. 1997. Evolution of genetic redundancy. Nature 388:167–171. https://doi.org/10.1038/40618.
48. Klappenbach JA, Dunbar JM, Schmidt TM. 2000. rRNA operon copy number reflects ecological strategies of bacteria. Appl Environ Microbiol 66:1328–1333. https://doi.org/10.1128/AEM.66.4.1328-1333.2000.
49. Mendonça AG, Alves RJ, Pereira-Leal JB. 2011. Loss of genetic redundancy in reductive genome evolution. PLoS Comput Biol 7:e1001082. https://doi.org/10.1371/journal.pcbi.1001082.
50. Kato S, Ohkuma M, Powell DH, Krepski ST, Oshima K, Hattori M, Shapiro N, Woyke T, Chan CS. 2015. Comparative genomic insights into ecophysiology of neutrophilic, microaerophilic iron oxidizing bacteria. Front Microbiol 6:1265. https://doi.org/10.3389/fmicb.2015.01265.
51. Field EK, Sczyrba A, Lyman AE, Harris CC, Woyke T, Stepanauskas R, Emerson D. 2015. Genomic insights into the uncultivated marine Zetaproteobacteria at Loihi Seamount. ISME J 9:857–870. https://doi.org/10.1038/ismej.2014.183.
52. McAllister SM, Polson SW, Butterfield DA, Glazer BT, Sylvan JB, Chan CS. 2020. Validating the Cyc2 neutrophilic iron oxidation pathway using metaomics of Zetaproteobacteria iron mats at marine hydrothermal vents. mSystems 5:e00553-19. https://doi.org/10.1128/mSystems.00553-19.
53. Croal LR, Johnson CM, Beard BL, Newman DK. 2004. Iron isotope fractionation by Fe(II)-oxidizing photoautotrophic bacteria. Geochim Cosmochim Acta 68:1227–1242. https://doi.org/10.1016/j.gca.2003.09.011.
54. Bethencourt L, Bochet O, Farasin J, Aquilina L, Borgne T, Quaiser A, Biget M, Michon-Coudouel S, Labasque T, Dufresne A. 2020. Genome reconstruction reveals distinct assemblages of Gallionellaceae in surface and subsurface redox transition zones. FEMS Microbiol Ecol 96:fiaa036. https://doi.org/10.1093/femsec/fiaa036.
55. Jeans C, Singer SW, Chan CS, VerBerkmoes NC, Shah M, Hettich RL, Banfield JF, Thelen MP. 2008. Cytochrome 572 is a conspicuous membrane protein with iron oxidation activity purified directly from a natural acidophilic microbial community. ISME J 2:542–550. https://doi.org/10.1038/ismej.2008.17.
56. Hädrich A, Taillefert M, Akob DM, Cooper RE, Litzba U, Wagner FE, Nietzsche S, Ciobota V, Rösch P, Popp J, Küsel K. 2019. Microbial Fe(II) oxidation by Sideroxydans lithotrophicus ES-1 in the presence of Schlöppnerbrunnen fen-derived humic acids. FEMS Microbiol Ecol 95:fiz034. https://doi.org/10.1093/femsec/fiz034.
57. Stookey LL. 1970. Ferrozine—a new spectrophotometric reagent for iron. Anal Chem 42:779–781. https://doi.org/10.1021/ac60289a016.
58. Riemer J, Hoepken HH, Czerwinska H, Robinson SR, Dringen R. 2004. Colorimetric ferrozine-based assay for the quantitation of iron in cultured cells. Anal Biochem 331:370–375. https://doi.org/10.1016/j.ab.2004.03.049.
59. Shi L, Liu J, Li N, Gao J. 2013. Chlorine dioxide-iodine-sodium thiosulfate oscillating reaction investigated by the UV-Vis spectrophotometric method. J Solution Chem 42:1207–1220. https://doi.org/10.1007/s10953-013-0028-4.
60. Bernstein JA, Khodursky AB, Lin P-H, Lin-Chao S, Cohen SN. 2002. Global analysis of mRNA decay and abundance in Escherichia coli at single-gene resolution using two-color fluorescent DNA microarrays. Proc Natl Acad Sci U S A 99:9697–9702. https://doi.org/10.1073/pnas.112318199.
61. Martin M. 2011. Cutadapt removes adapter sequences from high-throughput sequencing reads. EMBnetj 17:10–12. https://doi.org/10.14806/ej.17.1.200.
62. Langmead B, Salzberg SL. 2012. Fast gapped-read alignment with Bowtie 2. Nat Methods 9:357–359. https://doi.org/10.1038/nmeth.1923.
63. Li H, Handsaker B, Wysoker A, Fennell T, Ruan J, Homer N, Marth G, Abecasis G, Durbin R, 1000 Genome Project Data Processing Subgroup. 2009. The Sequence Alignment/Map format and SAMtools. Bioinformatics 25:2078–2079. https://doi.org/10.1093/bioinformatics/btp352.
64. Anders S, Pyl PT, Huber W. 2015. HTSeq—a Python framework to work with high-throughput sequencing data. Bioinformatics 31:166–169. https://doi.org/10.1093/bioinformatics/btu638.
65. Love MI, Anders S, Huber W. 2014. Differential analysis of count data—the DESeq2 package. Genome Biol 15:550–1184. https://doi.org/10.1186/s13059-014-0550-8.
66. Benjamini Y, Hochberg Y. 1995. Controlling the false discovery rate: a practical and powerful approach to multiple testing. J R Stat Soc Ser B 57:289–300. https://doi.org/10.1111/j.2517-6161.1995.tb02031.x.
67. Valero-Mora PM. 2010. ggplot2: elegant graphics for data analysis. J Stat Softw 35:1–3.

68. Yu NY, Wagner JR, Laird MR, Melli G, Rey S, Lo R, Dao P, Sahinalp SC, Ester M, Foster LJ, Brinkman FSL. 2010. PSORTb 3.0: improved protein subcellular localization prediction with refined localization subcategories and predictive capabilities for all prokaryotes. Bioinformatics 26:1608–1615. https://doi.org/10.1093/bioinformatics/btq249.
69. Rethmeier J, Rabenstein A, Langer M, Fischer U. 1997. Detection of traces of oxidized and reduced sulfur compounds in small samples by combination of different high-performance liquid chromatography methods. J Chromatogr A 760:295–302. https://doi.org/10.1016/S0021-9673(96)00809-6.
70. Chan L-K, Weber TS, Morgan-Kiss RM, Hanson TE. 2008. A genomic region required for phototrophic thiosulfate oxidation in the green sulfur bacterium Chlorobium tepidum (syn. Chlorobaculum tepidum). Microbiology 154:818–829. https://doi.org/10.1099/mic.0.2007/012583-0.